Photorefractive Polysilanes Functionalized with a Nonlinear Optical Chromophore

Eric Hendrickx, David Van Steenwinckel, and André Persoons*

Laboratory for Chemical and Biological Dynamics, Center for Research on Molecular Electronics and Photonics, University of Leuven, Celestijnenlaan 200D, B-3001 Leuven, Belgium

Akira Watanabe*

Institute for Chemical Reaction Science, Tohoku University, Katahira, Aoba-ku, Sendai 980-77, Japan

Received June 25, 1998; Revised Manuscript Received December 11, 1998

ABSTRACT: We have prepared various polysilane copolymers that were functionalized with the nonlinear optical chromophore *N*-methyl-*p*-nitroaniline. The glass transition temperature of the polysilanes was adjusted to room temperature by copolymerization of methylphenyldichlorosilane and *n*-hexylmethyldichlorosilane. Asymmetric two-beam coupling was observed at 633 nm, and a gain coefficient of 18 cm^{-1} was measured at an externally applied field of 48 V μm^{-1}.

Introduction

The photorefractive effect is described as a multistep process, involving the production of mobile charges, followed by charge transport through diffusion and drift. The free charges subsequently generate a space-charge field that modulates the refractive index.[1,2] It has been shown that the photorefractive effect can be used for the optical storage, exchange, and manipulation of information. The first materials shown to be photorefractive were inorganic crystals, such as $LiNbO_3$ and $BaTiO_3$. Recently, the photorefractive effect was also demonstrated in a variety of organic materials, such as polymer films,[3] liquid crystals,[4] and organic glasses.[5] Since organic materials are flexible, efficient, and inexpensive, they offer better perspectives for device commercialization than the traditional crystals.

The components of organic photorefractive polymer films reflect the multistep buildup of a photorefractive grating; i.e., they mostly are polymer composites with a sensitizer (charge generator), photoconductor (charge transport agent), and a nonlinear optical dye for the modulation of the refractive index. This approach has led to the development of polymer films with high diffraction efficiency and two-beam coupling gain.[6,7] Frequently, the photorefractive films are polymer composites of the photoconductor poly(vinylcarbazole), the plasticizer and photoconductor ethylcarbazole, a highly polar, nonlinear optical, chromophore, and a small amount of sensitizer. A drawback of this approach is the phase instability of the composite. Because of the incompatibility of the apolar photoconductor and the polar dye, the photorefractive films often show phase separation, on a time scale from several weeks to several months, due to the crystallization of the dye.[8,9] While the phase stability of a polymer composite can be improved by, for example, using a eutectic dye mixture, fully functionalized polymers offer the best perspectives in terms of stability.[10] Therefore, in this work, we study polysilanes functionalized with a polar dye, *N*-methyl-*p*-nitroaniline (NMPNA).

Polysilanes are semiconducting polymers that show σ-conjugation along the Si−Si main chain. A high photoconductivity has been reported for linear polysilanes.[11−15] Only holes were found to be mobile, and a mobility of 10^{-4} $cm^2/(V\ s)$, approximately 4 orders of magnitude higher than that of poly(vinylcarbazole), was measured. Polysilane-based high-mobility photorefractive materials were first reported by Silence and coworkers.[16,17] Poly(4-*n*-butoxyphenylethylsilane) was used as a host polymer. To achieve optical nonlinearity, a nonlinear optical (NLO) chromophore, such as a coumarin-150, was added to the polymer as a dopant. A small amount of 2,4,7,-trinitro-9-fluorenone (TNF) or fullerene C_{60} was also included as a charge generator. The poly(4-*n*-butoxyphenylethylsilane) has a low glass transition temperature ($T_g = 55$ °C) and relatively polar side groups (butoxy group), which enhance the dispersion of chromophores in the host polymer. Gain coefficients on the order of 0.2−1.7 cm^{-1} were observed, along with steady-state diffraction efficiencies of 10^{-4} and response times as fast as 39 ms. These data clearly show the good potential for polysilanes as hole transport agents in photorefractive materials.

In this paper, we report on the synthesis and characterization of polysilanes with a nonlinear optical chromophore in the side chain. This is a new class of charge transporting host polymer functionalized with an NLO group. To lower the glass transition temperature of the polymer to room temperature and to enhance the index modulation by birefringence, the polysilane main chain was a copolymer of methylphenyldichlorosilane and hexylmethyldichlorosilane. NMPNA was covalently attached to the polysilane main chain. Two-beam coupling measurements were done at 633 nm and showed that the polymer is photorefractive.

Results and Discussion

Synthesis and Characterization of NLO Polysilanes. Polysilanes with an NLO chromophore in the side chain were synthesized by functionalizing a polysilane to avoid interference of the reactive groups of the NLO chromophores, such as the amino group, during the polymerization. Organodichlorosilanes, functionalized with an amino group, are unstable in the synthesis and the polymerization by a Wurtz type reaction. A chloromethylated polysilane is a convenient

10.1021/ma9810013 CCC: $18.00
Published on Web 03/11/1999

Scheme 1. Synthetic Routes for Polysilanes Functionalized with *N*-Methyl-*p*-nitroaniline[a]

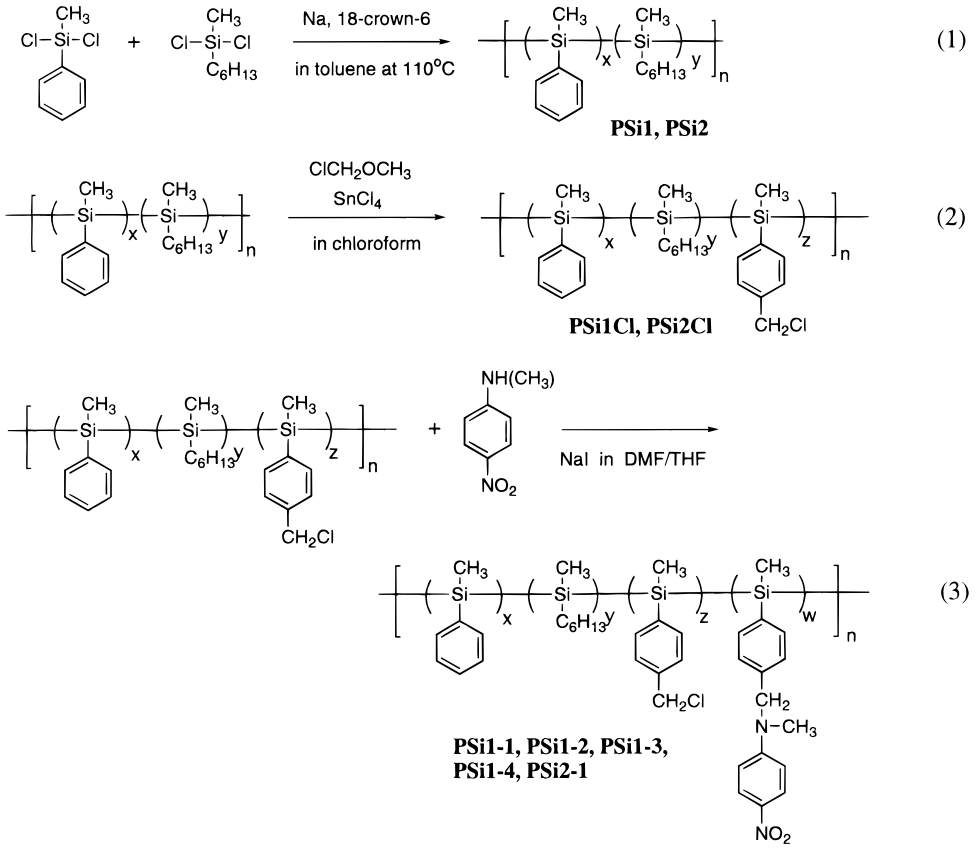

[a] Note that although the chloromethylated group is represented in the para position of the phenyl group, its actual position can be either the para or ortho position.[18]

Table 1. Composition and Molecular Weight of the Synthesized Polysilanes

polymer	*x*	*y*	*z*	*w*	M_w	M_w/M_n
PSi1	0.43	0.57			8 600	4.94
PSi2	0.83	0.17			5 100	3.07
PSi1Cl	0.12	0.57	0.31		28 500	6.38
PSi2Cl	0.02	0.17	0.81		15 600	5.91
PSi1−1	0.12	0.57	0.00	0.31	11 200	2.59
PSi1−2	0.12	0.57	0.10	0.21	26 100	4.94
PSi1−3	0.12	0.57	0.19	0.12	45 200	7.75
PSi1−4	0.12	0.57	0.24	0.07	11 600	3.51
PSi2−1	0.02	0.17	0.00	0.81	32 300	4.07

polymer for the modification of the side chain. The synthesis of the chloromethylated poly(methylphenylsilane) has been reported by Ban and co-workers.[18] To lower the T_g, we carried out the copolymerization of methylphenyldichlorosilane with *n*-hexylmethyldichlorosilane. Polysilanes with a long alkyl chain as a side group have a low T_g value because of the flexibility of the alkyl chain. Although poly(di-*n*-hexylsilane) is a typical alkyl-substituted polysilane with a melting point of 42 °C,[19] it has a crystalline structure because of the symmetric substitution of the Si main chain. Therefore, we chose an asymmetric unit, such as *n*-hexylmethylsilane, in the copolymerization to reduce the crystallinity and to improve the transparency. The poly(hexylmethylsilane) is an oily substance at room temperature. The synthetic routes are depicted in Scheme 1. We have prepared two kinds of polysilanes as base polymers, PSi1 and PSi2, where the ratios of the feed monomer (methylphenyldichlorosilane/*n*-hexylmethyldichlorosilane) were 1/1 and 4/1, respectively. The composition of the copolymers was determined by the integration of the signals of the alkyl protons around 1 ppm and the aromatic protons around 7 ppm in the ^{1}H NMR spectra. The results are summarized in Table 1. The ratio of the phenyl-substituted Si unit to the alkyl-substituted Si unit in the copolymer is almost similar to the feed composition. PSi1, with the smallest content of phenyl groups, is an oily substance at room temperature while PSi2, with the largest content of phenyl groups, is a white powder. The chloromethylated polymers of PSi1 and PSi2 are abbreviated by PSi1Cl and PSi2Cl, respectively, and the ratios of chloromethylation are summarized in Table 1. These ratios were determined by the integration of the signals of the alkyl protons (CH_2Cl) at 4.51 ppm and the aromatic protons around 7 ppm in the ^{1}H NMR spectra. In Scheme 1, although the position of the chloromethyl group is represented in the para position of the phenyl group, it can be placed both in the para and ortho position by the Friedel−Crafts reaction.[18]

Because PSi1 and PSi1Cl are oily polymers, we measured the molecular weight distribution using a GPC system equipped with columns for molecular weights lower than 100 000. Figure 1 shows the elution

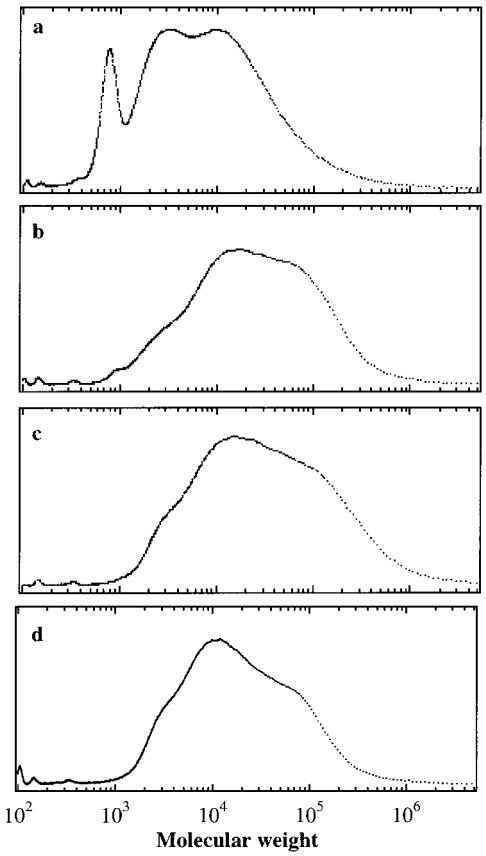

Figure 1. GPC elution curves of PSi1 (a), PSi1Cl (b), PSi1−3 (c), and PSi1−2 (d).

curves of PSi1, PSi1Cl, PSi1−2, and PSi1−3. In the elution curves, the region where the molecular weight is higher than 100 000 corresponds to the exclusion limit of the GPC columns. In Figure 1, there is no oligomer component for PSi1Cl, PSi1−2, and PSi1−3 while PSi1 shows a sharp oligomer peak. The oligomer components of PSi1 can possibly be attributed to cyclic silicon compounds.[20−23] These oligomer components were also observed in the elution curve of PSi2. However, the elution curves of the other polymers do not show oligomer components. The oligomer components of PSi1 and PSi2 are removed by the precipitation in methanol after the substitution reactions. Hence, the oily appearance of PSi1Cl is not due to the plasticization of the polymer by low molecular weight components, but it is caused by the asymmetric substitution with long alkyl chains.

Table 1 shows the molecular weights that were determined by GPC using monodisperse polystyrene as standards. The molecular weights of the polysilanes increase by linking the Cl group or the NMPNA group to the side chain. Substitution with polar and bulky groups causes deviation of the molecular weight from the calibration curves determined using polystyrenes. It is also possible that some cross-linking during the substitution reaction increases the molecular weight. Actually, in the formation of PSi1−1 by the reaction of PSi1 with NMPNA, 70% of the reaction products are insoluble. Note that this reaction was carried out at 110 °C, the highest temperature used in the functionalization reactions. The cross-linking may be caused by the reaction of the amino group of the NMPNA side chain with a chloromethyl group of another side chain.

Table 2. Glass Transition Temperatures and Degradation Temperatures of the Synthesized Polysilanes in °C

polymer	T_g	T_d	polymer	T_g	T_d
PSi1		>200	PSi1−2	35	97
PSi2		>200	PSi1−3	35	160
PSi1Cl	−28	>200	PSi1−4	−10	139
PSi2Cl	42	>200	PSi2−1	98	97
PSi1−1	40	154			

The glass transition temperatures T_g and decomposition temperatures T_d were determined using a modulated DSC and are summarized in Table 2. For high-T_g materials, the mechanism for the refractive index modulation is the linear electrooptic effect, or Pockels effect. If the T_g of a photorefractive material is close to room temperature, the modulation of the refractive index is enhanced by birefringence because the nonlinear optical chromophores can reorient.[24,25] Therefore, in the high-performance photorefractive polymers developed so far, the T_g is lowered to room temperature by the addition of a plasticizer. Here we fine-tune the T_g of the polymer by copolymerization of a high-T_g and low-T_g polysilane. The T_g values of PSi1 and PSi2 are −40 and 43 °C, respectively. The T_g values of the polysilanes are not significantly increased by the chloromethyl group.

The glass transition temperature T_g has to increase by the addition of a large NLO group to the polysilane side chain. We have prepared NLO polysilanes with different degrees of functionalization and have measured the T_g values. By changing the reflux temperature, the ratios of the NMPNA group were controlled. The NLO polysilanes PSi1−1, PSi1−2, PSi1−3, PSi1−4, and PSi2−1 were obtained by the reactions at 110, 80, 70, 60, and 100 °C, respectively. The content of the NMPNA group was determined by the integration of the signals of the alkyl protons (phenyl−CH_2Cl at 4.51 ppm, phenyl−CH_2−N at 4.39 ppm) and methyl protons (CH_3−N at 3.14 ppm). As shown in Table 2, T_g becomes higher with increasing content of NMPNA groups. The direct functionalization of the apolar polymer Si backbone with polar NLO molecules also leads to an improvement in phase stability, compared to composites of nonfunctionalized polysilanes doped with NLO molecules. To test the stability improvement obtained by using a functionalized copolymer, we have tried to prepare polymer composite samples of PSi1Cl doped with NMPNA. This polymer composite crystallized immediately, which illustrates the improved phase behavior of the functionalized polymer.

The use of a modulated DSC allows to distinguish between processes that are reversible or irreversible on the time scale of the modulation. The total heat flow is split up in a reversible and an irreversible component. The reversible and irreversible heat flow components for PSi1−2 are shown in Figure 2, a and b, respectively. Each curve has a specific feature. The reversible curve shows a glass transition temperature around 35 °C. The irreversible curve has an exothermal transition starting around 75 °C. Since beyond this transition the material changes color from yellow to black and becomes brittle, we take this temperature to be the onset of degradation. The degradation temperature listed in Table 2 is the temperature at the intersection of the lines tangential to the DSC curve before and after the degradation onset. We did not exceed this temperature during the photorefractive sample preparation. In Figure 3 the T_g values are plotted against the normalized content of phenyl

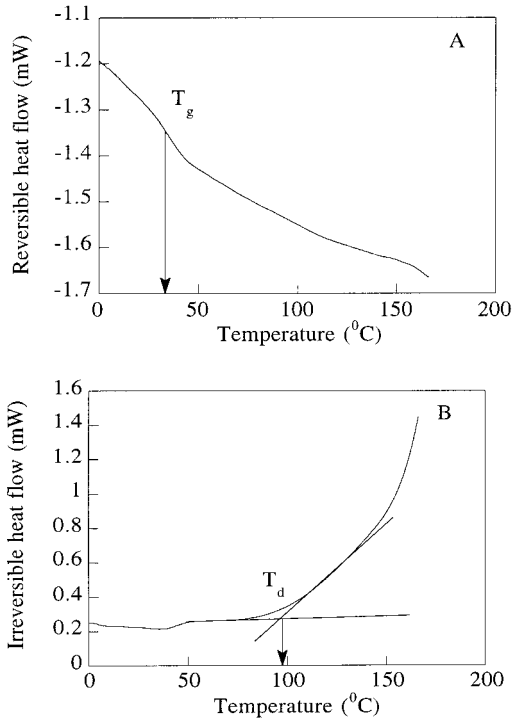

Figure 2. MDSC results obtained during a heating scan on PSi1−2 at an underlying heating rate of 5 °C/min. The direction of exothermal changes is upward for both curves. (A) Reversible heat flow. This component shows a T_g at 35 °C. (B) Nonreversible heat flow. There is an exothermal degradation reaction starting at 75 °C. The degradation temperature was determined by linear extrapolation of the curve before and after the degradation onset and is 97 °C.

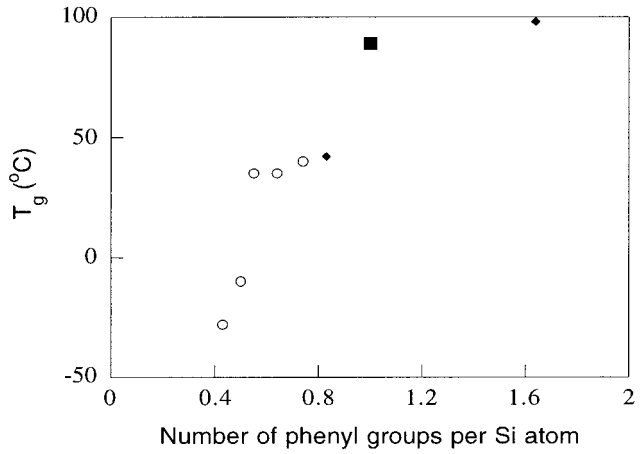

Figure 3. Dependence of T_g on normalized content of phenyl group: circle, PSi1-based polymers; diamonds, PSi2-based polymers; square, poly(methylphenylsilane).

groups. The number of phenyl groups per Si unit was obtained by the equation $x + z + 2w$, where x, z, and w are related to the stoichiometric phenyl content of the copolymer (Scheme 1). The T_g shows good correlation with the normalized content of phenyl groups for NLO polysilanes from PSi1 (circles) and from PSi2 (diamond). In Figure 3, the T_g value of poly(methylphenylsilane) is also plotted (square) and agrees with the other data.

Optical Properties. Polysilanes show a characteristic absorption band in the UV−visible region due to the σ-conjugation along the Si−Si main chain. Figure 4 shows the absorption spectra of PSi1, PSi2, and the chloromethylated polysilanes. The absorption maxima of PSi1 at 321 and 270 nm can be assigned to the $\sigma-\sigma^*$

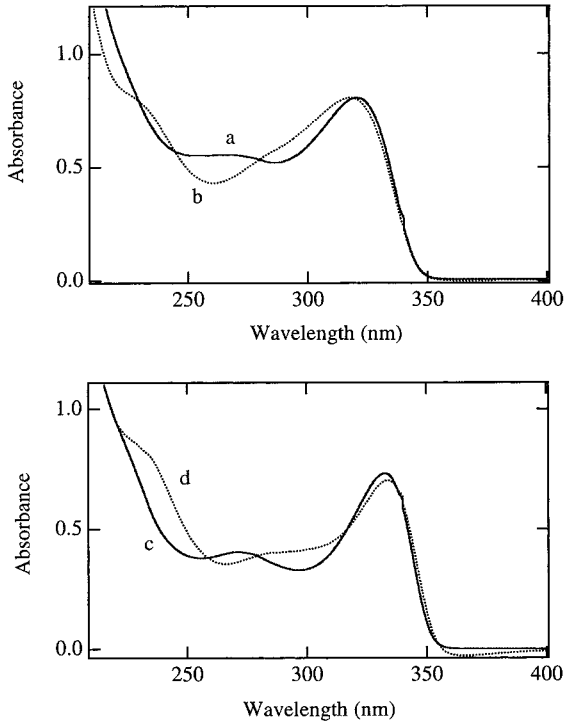

Figure 4. Absorption spectra of polysilane copolymers and the chloromethylated polysilanes in THF: (a) PSi1, (b) PSi1Cl, (c) PSi2, and (d) PSi2Cl.

transition of σ-conjugated Si−Si main chain and the $\pi-\pi^*$ transition of the phenyl group, respectively. By substitution of a phenyl proton with a chloromethyl group, the $\sigma-\sigma^*$ transition shows only a small blue shift, from 321 to 319 nm, and remains dominant. The $\pi-\pi^*$ band, however, is strongly affected. PSi2 also shows $\sigma-\sigma^*$ and $\pi-\pi^*$ bands at 333 and 273 nm, respectively. PSi2 shows no blue shift of the $\sigma-\sigma^*$ band by the introduction of the chloromethyl group. These results suggest that the σ-conjugation of polysilane copolymers is not affected by chloromethylation.

Figure 5A shows the absorption spectra of polysilanes with various NMPNA substitution ratios, PSi1−1, PSi1−2, PSi1−3, and PSi1−4. The absorbance is normalized at the absorption maximum of the $\sigma-\sigma^*$ band. The absorption maximum of the $\sigma-\sigma^*$ band does not change by varying the NMPNA content. This suggests that there is no conjugation between the Si−Si main chain and the NMPNA side chain. The absorption maximum of PSi1−1 at 386 nm is attributed to the NMPNA group attached to the phenyl side chain. The absorption maximum shows a red shift compared to that of NMPNA at 376 nm, which is induced by the electron-donating effect from the phenyl side chain. In Figure 5B, the absorption spectrum of PSi2−1, with a high NMPNA content, is compared to the spectrum of PSi2. In this case, the $\sigma-\sigma^*$ band of PSi2−1 shows a slight red shift, from 333 to 337 nm. This red shift may be caused by a conformational change of the Si−Si main chain, induced by the bulky NMPNA groups in the side chain. The bulkiness of the side chains changes a coillike conformation into a rodlike conformation. The rodlike conformation enhances the $\sigma-\sigma^*$ conjugation along the Si−Si main chain and causes the red shift of the absorption band.[19]

In Figure 6, the absorption spectrum of the NMPNA-substituted polysilane film is compared with a concentrated solution of NMPNA in THF. In the absorption

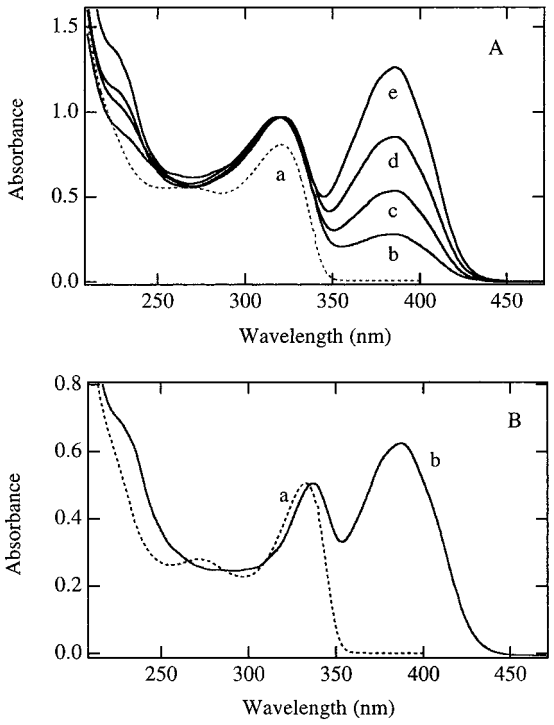

Figure 5. Absorption spectra of polysilanes with various NMPNA substitution ratio in THF. (A) PSi1-based polymers: (a) PSi1, (b) PSi1−1, (c) PSi1−2, (d) PSi1−3, and (e) PSi1−4. (B) PSi2-based polymers: (a) PSi2 and (b) PSi2−1.

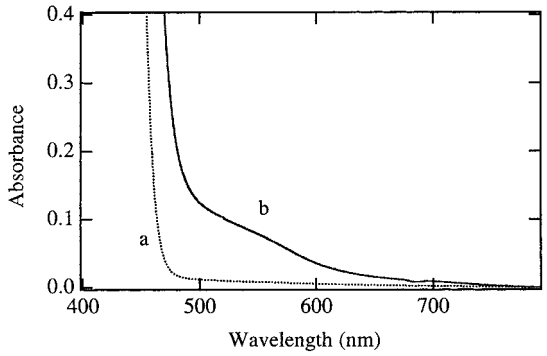

Figure 6. Absorption spectra of (a) NMPNA in THF (100 mM, 2 mm optical path length) and (b) PSi1−2 film (ca. 0.02 mm thickness). The absorption coefficient of PSi1−2 was determined to be 21 cm^{-1}.

spectrum of NMPNA, there is no absorption band at wavelengths higher than 500 nm. On the other hand, the PSi1−2 film shows a broad absorption band around 550 nm. Possibly this absorption is produced by a complexation between NMPNA and the σ-conjugated Si main chain.

Photorefractive Measurements. The photorefractive response of a material can be verified by asymmetric two-beam coupling experiments.[26,27] The nonlocal response or the phase shift between the index grating and the intensity pattern leads to an energy exchange between the two writing beams incident on the sample. It is a signature of a photorefractive index grating and distinguishes a photorefractive index grating from other laser-induced dynamic gratings, such as a photochromic grating.

The voltage applied over the sample was increased from 0 to 6 kV by increments of 1 kV every 10 min. We verified that reversing the polarity of the applied voltage leads to a reversal in the direction of the energy transfer, which proves the asymmetry of the two-beam coupling. The gain coefficient as a function of electric field for the photorefractive samples was calculated from the observed energy exchange and is shown in Figure 7.

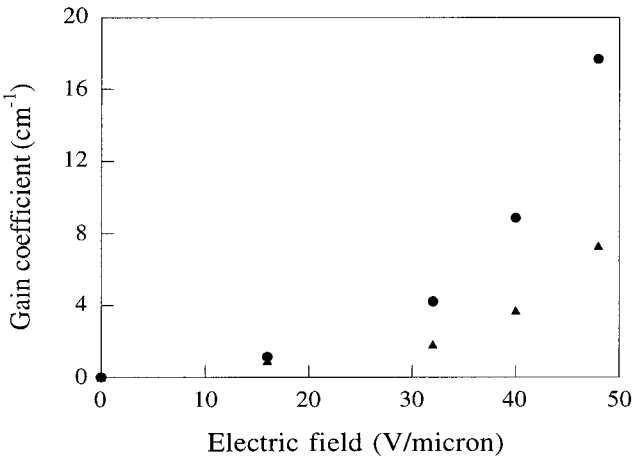

Figure 7. Asymmetric two-beam coupling gain coefficient as a function of applied electric field for PSi1−2 and PSi1−3: circles, PSi1−2; triangles, PSi1−3. The writing beams were p-polarized.

The Γ values for PSi1−2 are larger than the Γ values for PSi1−3. Since, according to the coupled-wave equations, Γ is related to both the phase shift θ (between the intensity pattern and the index pattern) and the index modulation amplitude Δn[26]

$$\Gamma = \frac{4\pi}{\lambda}(\bar{e}_1 \cdot \bar{e}_2^*)\Delta n \sin\theta \qquad (1)$$

where $\bar{e}_i$ are the polarization vectors of the incoming beams. The NMPNA loading of PSi1−2 (21%) is larger than that of PSi1−3 (12%) and hence should have a larger Δn value according to the oriented gas model. Assuming a similar value for the phase shift in both materials, this can possibly explain the increased efficiency for PSi1−2.

The photorefractive polysilane polymer composites described in ref 16 had gain coefficients of the order of 0.2−2 cm^{-1} at applied electric fields of about 11 V/μm. Due to the higher applied fields here, the gain coefficient of PSi1−2 peaks at 18 cm^{-1}, which represents an improvement by 1 order of magnitude. In our experimental geometry, a gain of 18 cm^{-1} corresponds to 13% energy transfer between the writing beams. A difference with the polysilane composites in ref 16 is the speed of the buildup. PSi1−2 and PSi1−3 only reached a steady state after buildup times of several minutes, compared to rise times of 40 ms for the composites. Possibly this is due to a reduced photogeneration efficiency or slow photogeneration.

We have also tested the photorefractive two-beam coupling response of a sample of PSi1−2 sensitized with 0.02 wt % C_{60}. A high photoconductivity has been reported for fullerene-doped polysilanes.[28,29] The charges are generated by the electron transfer between polysilane and C_{60}.[30] However, the Γ value and the response time of PSi1−2 did not improve by the addition of C_{60}. In our photorefractive measurements, a He−Ne laser (633 nm) was used for the excitation of C_{60}-doped PSi1−2. The absorption spectrum of the C_{60}-doped PSi1−2 film does not show a CT band due to complexation with C_{60} at that wavelength. In this case, C_{60} is directly

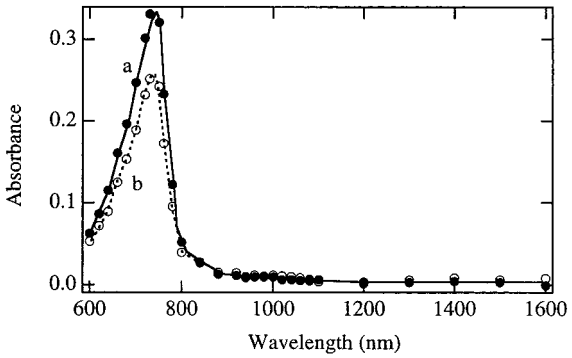

Figure 8. Transient absorption spectra obtained by 532 nm laser pulse excitation of 0.1 mM C_{60} in deaerated benzonitrile in the presence of 5 mM PSi1−2: (a) 100 ns, (b) 1000 ns.

excited by the laser beam, and an electron transfer from polysilane to the C_{60} excited state is necessary for charge generation. The charge generation via excited-state C_{60} is less efficient compared to that via excited-state polysilane. The electron-transfer reaction between PSi1−2 and C_{60} was examined by laser flash photolysis. Figure 8 shows the transient absorption spectra obtained by 532 nm laser pulse excitation of C_{60} in benzonitrile solution in the presence of PSi1−2. The transient absorption at 730 nm is assigned to C_{60} triplet excited state. There is no absorption band of a radical ion generated by the electron transfer between C_{60} and PSi1−2. This is in contrast with poly(methylphenylsilane), which shows the formation of a poly(methylphenysilane) radical cation and a C_{60} radical anion by a photoinduced electron-transfer reaction,[30] and explains why C_{60} does not work as a sensitizer for PSi1−2 in the photorefractive measurements. The photoinduced electron transfer from the polysilane Si−Si bond to C_{60} is possibly reduced by the electron-withdrawing nitro group of the PSi1−2 side chain.

Conclusion

In summary, we have prepared new photorefractive materials based on polysilane polymers. A total of five copolymers functionalized with the nonlinear optical chromophore *N*-methyl-*p*-nitroaniline were synthesized. The glass transition temperature was lowered to room temperature by copolymerization and was found to correlate with the number of phenyl units per silicon atom. The UV−vis spectra do not suggest that the Si−Si σ-conjugation is affected by the substitution.

Asymmetric two-beam coupling was observed for PSi1−2 and PSi1−3, demonstrating the presence of a photorefractive grating. A gain coefficient of 18 cm^{-1} was measured at 633 nm for PSi1−2 at an applied electric field of 48 V/μm.

Experimental Section

Materials. We have prepared two kinds of polysilanes, by a Wurtz coupling reaction, as base polymers, PSi1 and PSi2, where the ratios of the feed monomer (methylphenyldichlorosilane/*n*-hexylmethyldichlorosilane) were 1/1 and 4/1, respectively. The synthesis was done as follows:[31] A 300 mL three-neck flask was fitted with reflux condenser, a pressure-equalized dropping funnel, and a motor-driven stirrer. The system was purged with nitrogen. Dry toluene (80 mL), sodium (184 mmol), and 18-crown-6 (3 mmol) were added to the flask, and the flask was heated to 110 °C under rapid stirring to create a sodium dispersion. Methylphenyldichlorosilane (40 mmol) and *n*-hexylmethyldichlorosilane (40 mmol), diluted with dry toluene (10 mL), were added dropwise to the sodium dispersion. The mixture was refluxed while stirring at 110 °C for 1 h. Then the reaction vessel was cooled to room temperature, and the mixture was separated into a supernatant solution and an inorganic precipitate by centrifugation. The supernatant fraction was slowly added to methanol with stirring, and PSi1 was obtained as a white precipitate. The yield was 26.3%, based on the Si unit. PSi2 was obtained by a similar procedure, using methylphenyldichlorosilane (16 mmol) and *n*-hexylmethyldichlorosilane (64 mmol). The yield was 21.3% based on the Si unit.

The chloromethylated polysilanes PSi1Cl and PSi2Cl were prepared by a procedure similar to that of Ban and coworkers.[18] A polysilane (1 g) was dissolved in a mixture of 10 mL of chloromethyl methyl ether and 10 mL of chloroform. $SnCl_4$ (1 g) was slowly dropped to the solution at 0 °C under nitrogen. After stirring for 20 h at 5 °C, the solution was dropped into methanol to obtain the chloromethylated polysilane. The yield of the reaction was about 60% based on the Si unit.

The reaction of chloromethylated polysilane with NMPNA was carried out as follows: A chloromethylated polysilane (3 mmol, based on the Si units) and NMPNA (6 mmol) were dissolved into a mixture of 10 mL of *N*,*N*-dimethylformamide (DMF) and 10 mL of tetrahydrofuran (THF) with NaI (30 mmol). The solution was refluxed for 12 h with stirring under nitrogen. The ratio of substitution of the Cl groups with the NMPNA groups was controlled by changing the reflux temperature. The solution was dropped into a methanol/water mixed solvent. The polymer was further purified by reprecipitation using a methanol/water mixed solvent.

Samples for photorefractive measurements were prepared by flattening a small amount of polymer (60 mg) at 60−70 °C between a glass and Teflon slide. Then the material was cooled to 0 °C, and the slides were separated. Small pieces of the polymer were cut and put on two ITO-covered glass slides. The glass slides were heated to 70 °C and pressed together. Stripped optical fiber was used as spacer to ensure a uniform sample thickness of 125 μm. Samples were prepared of PSi1−2 and PSi1−3.

Measurements. NMR spectra were recorded using a JEOL GX-400 spectrometer. The GPC elution curves were determined by a Waters HPLC system equipped with columns GPC KF-802.5 (Shodex) and TSKgel G2000H (TOSOH). The number-average molecular weight (M_n) and the molecular weight distribution (M_w/M_n) were determined by a calibration curve using monodispersed polystyrene as standards. DSC scans were performed using a modulated DSC with an underlying heating rate of 5 °C/min. The oscillation period was 60 s, and the oscillation amplitude was ±0.8 °C. The amount of material used was 7−9 mg for all polymers.

Two-beam coupling measurements were done using an experimental geometry and setup similar to the one described in ref 32. The laser was a He−Ne laser operating at 633 nm. The angle between the two writing beams outside the sample was 27°, and the angle between the bisector of the writing beams and the surface normal was 60°. The two beams were p-polarized, had a power of 0.2 mW each, and were collimated to 500 μm diameter in the sample. The analysis of the data was done using the equation

$$\Gamma d = \cos\alpha_1 \ln\left(\frac{I_1^t\,(I_2 \neq 0)}{I_1^t\,(I_2 = 0)}\right) - \cos\alpha_2 \ln\left(\frac{I_2^t\,(I_1 \neq 0)}{I_2^t\,(I_1 = 0)}\right) \quad (2)$$

I_1^t and I_2^t are the transmitted intensities of writing beams 1 and 2. Beam 1 is the beam closest to the surface normal, α_1 and α_2 are the angles between the writing beams and the surface normal in the sample, d is the sample thickness, and Γ is the gain coefficient. The values for α_1 (25.2°) and α_2 (34.3°) were calculated using an estimated refractive index of 1.7 for the polysilane copolymers.

Acknowledgment. E.H. is a Research Associate and D.V.S. a research assistant of the Fund for Scientific

Research−Flanders (FWO-V, Belgium). This research was supported by research grants from the FWO-V (G.0308.96), from the Belgian government (IUAP P4/11, "Supramolecular Chemistry and Supramolecular Catalysis"), and from the University of Leuven (GOA/95/01). This work was partially supported by a Grant-in-Aid for Scientific Research No. 09650984 from the Ministry of Education, Science and Culture, Japan.

References and Notes

(1) Günter, P.; Huignard, J.-P. In *Photorefractive Materials and Their Applications*; Springer-Verlag: Berlin, 1988−1989; Vols. I and II.
(2) Kukhtarev, N. V.; Markov, V. B.; Odulov, S. G.; Soskin, M. S.; Vinetskii, V. L. *Ferroelectrics* **1979**, *22*, 949.
(3) Ducharme, S.; Scott, J. C.; Twieg, R. J.; Moerner, W. E. *Phys. Rev. Lett.* **1991**, *66*, 1846.
(4) Wiederrecht, G. P.; Yoon, B.; Wasielewski, M. R. *Science* **1995**, *270*, 1794.
(5) Lundquist, P. M.; Wortmann, R.; Geletneky, C.; Twieg, R. J.; Jurich, M.; Lee, V. Y.; Moylan, C. R.; Burland, D. M. *Science* **1996**, *274*, 1182.
(6) Meerholz, K.; Volodin, B. L.; Sandalphon; Kippelen, B.; Peyghambarian, N. *Nature* **1994**, *371*, 497.
(7) Kippelen, B.; Marder, S. R.; Hendrickx, E.; Maldonado, J. L.; Guillemet, G.; Volodin, B. L.; Steele, D. D.; Enami, Y.; Sandalphon; Yao, Y. J.; Wang, J. F.; Röckel, H.; Erskine, L.; Peyghambarian, N. *Science* **1998**, *279*, 54.
(8) Hendrickx, E.; Volodin, B. L.; Steele, D. D.; Maldonado, J. L.; Wang, J. F.; Kippelen, B.; Peyghambarian, N. *Appl. Phys. Lett.* **1997**, *71*, 1159.
(9) Meerholz, K.; Bittner, R.; De Nardin, Y.; Bräuchle, C.; Hendrickx, E.; Volodin, B. L.; Kippelen, B.; Peyghambarian, N. *Adv. Mater.* **1997**, *9*, 1043.
(10) Yu, L.; Chan, W. K.; Peng, Z.; Gharavi, A. *Acc. Chem. Res.* **1996**, *29*, 13.
(11) West, R.; David, L. D.; Djurovich, P. I.; Stearley, K. L.; Srinivasan, K. S. V.; Yu, H. *J. Am. Chem. Soc.* **1981**, *103*, 7352.
(12) West, R. *J. Organomet. Chem.* **1986**, *300*, 327.
(13) Kepler, R. G.; Zeiglar, J. M.; Harrash, L. A.; Kurtz, S. R. *Phys. Rev. B* **1987**, *35*, 2818.
(14) Fujino, M. *Chem. Phys. Lett.* **1987**, *136*, 451.
(15) Stolka, M.; Yuh, H.-J.; McGrane, K.; Pai, D. M. *J. Polym. Sci., Polym. Chem. Ed.* **1987**, *25*, 823.
(16) Silence, S. M.; Scott, J. M.; Hache, F.; Ginsburg, E. J.; Jenkner, P. K.; Miller, R. D.; Twieg, R. J.; Moerner, W. E. *J. Opt. Soc. Am. B* **1993**, *10*, 2306.
(17) Moerner, W. E.; Silence, S. M. *Chem. Rev.* **1994**, *94*, 127.
(18) Ban, H.; Sukegawa, K.; Tagawa, S. *Macromolecules* **1987**, *20*, 1775.
(19) Miller, R. D.; Hofer, D.; Rabolt, J.; Fickes, G. N. *J. Am. Chem. Soc.* **1985**, *107*, 2172.
(20) Carberry, E.; West, R. *J. Organomet. Chem.* **1966**, *6*, 583.
(21) Laguerre, M.; Dunogues, J.; Calas, R. *J. Chem. Soc., Chem. Commun.* **1978**, 272.
(22) Matsumura, K.; Brough, L. F.; West, R. *J. Chem. Soc., Chem. Commun.* **1978**, 1092.
(23) Gilman, H.; Atwell, W. H.; Cartledge, F. K. *Adv. Organomet. Chem.* **1966**, *4*, 1.
(24) Wu, J. W. *J. Opt. Soc. Am. B* **1991**, *8*, 142.
(25) Moerner, W. E.; Silence, S. M.; Hache, F.; Bjorklund, G. C. *J. Opt. Soc. Am. B* **1994**, *11*, 320.
(26) Kippelen, B.; Meerholz, K.; Peyghambarian, N. In *Nonlinear Optics of Organic Molecules and Polymers*; Nalwa, H. S., Miyata, S., Eds.; CRC Press: Boca Raton, FL, 1997; p 482.
(27) Grunnet-Jepsen, A.; Thompson, C. L.; Moerner, W. E. *J. Opt. Soc. Am.* **1998**, *15*, 905.
(28) Wang, Y.; West, R.: Yuan, C.-H. *J. Am. Chem. Soc.* **1993**, *115*, 3844.
(29) Kepler, R. G.; Cahill, P. A. *Appl. Phys. Lett.* **1993**, *63*, 1552.
(30) Watanabe, A.; Ito, O. *J. Phys. Chem.* **1994**, *98*, 7736.
(31) Watanabe, A.; Matsuda, M. *Macromolecules* **1992**, *25*, 484.
(32) Volodin, B. L.; Sandalphon; Meerholz, K.; Kippelen, B.; Kukhtarev, N. V.; Peyghambarian, N. *Opt. Eng.* **1995**, *34*, 2213.

MA9810013